MODELLING THE CUTTING FORCES IN MICRO END MILLING USING A HYBRID APPROACH

Xiubing Jing[1,2], Huaizhong Li[2*], Jun Wang[2], and Yanling Tian[1]
[1] Key Laboratory of Advanced Ceramics and Machine Technology of Ministry of Education, TianJin University, Tianjin 300072, China
[2] School of Mechanical and Manufacturing Engineering, The University of New South Wales, Sydney, NSW 2052, Australia

Abstract

This paper presents the development of a cutting force model for the micro end milling processes under various cutting conditions using a hybrid approach. Firstly a finite element (FE) model of orthogonal micro-cutting with a round cutting edge is developed for a medium-carbon steel. A number of finite element analyses (FEA) are performed at different uncut chip thicknesses and velocities. Based on the FEA results, the cutting force coefficients are extracted through a non-linear algorithm to establish a relationship with the uncut chip thickness and cutting speed. Then the cutting force coefficients are integrated into a mechanistic cutting force model, which can predict cutting forces under different cutting conditions. In order to account for the cutting edge effect, an effective rake angle is employed for the determination of the cutting force. A comparison of the prediction and experimental measured cutting forces has shown that the developed method provides accurate results.

Keyword

Micro-end-milling; cutting force; micromachining; tool edge radius; modeling; metal cutting

[*] Corresponding author. Phone: +61-2-9385 5587; Fax: +61-2-9663 1222; E-mail: lihuaizhong@gmail.com ; hz.li@unsw.edu.au (Huaizhong Li)

Nomenclature

A, B, C, n, m	material constants in Johnson-Cook constitutive model
d_a	axial depth of cut (mm)
e_{ri}	runout of its *i*-th tooth relative to nominal tool radius
f	feed rate (mm/s)
f_t	feed per tooth (mm/tooth)
F_t, F_r, F_a	cutting forces in the tangential, radial and axial directions (N)
h, h_{tr}	uncut chip thickness (mm)
h_{lim}	limit value of the uncut chip thickness (mm)
i, j, k	indices for flutes, angular position, and axial disk element, respectively
K_{tc}, K_{rc}, K_{ac}	cutting force coefficients in tangential, radial and axial directions (N/mm^2)
K_{te}, K_{re}, K_{ae}	edge force coefficients in tangential, radial and axial dirctions (N/mm)
N_t	number of teeth of the milling cutter
R	radius of end-milling cutter (mm)
t	time (s)
T, T_m, T_{room}	temperature, melting temperature, and room temperature
V	cutting speed(m/min)
α , α_e	rake angle, effective rake angle
β	tool helix angle (deg)
β_n	friction angle
η	chip flow angle (deg)
$\theta(j)$	cutter rotation angle at simulation index j (deg)
ρ	tool cutting edge radius

ω spindle angular velocity(rad/s)

ϕ_n normal shear angle

ϕ_j the instantaneous position angle of the tooth tip analyzed

ε, $\dot{\varepsilon}$, $\dot{\varepsilon}_0$ equivalent strain, equivalent strain rate, and reference strain rate

τ_s shear yield stress

1 Introduction

Micro-milling operation is widely used to fabricate miniaturised components with complex 3D (three-dimentional) geometries and shapes in biomedical, optics and electronics industries [1, 2]. Modeling of the cutting forces in micro-milling is important for process planning and optimization. Since the chip thickness in micro-milling is of the order of 0.5 to 5 μm, which is comparable to the tool edge radius, the tool is not seen a sharp cutting edge. As a result, the cutting edge is rubbing or ploughing the workpiece rather than cutting, causing a significant increase of cutting forces as the frictional forces are increased. The strong size effect makes prediction of the cutting forces more challenging [3]. It is therefore important to study the mechanics of micro cutting processes, and develop comprehensive cutting force models.

There have been extensive research efforts on understanding the mechanics in micro-milling process and developing comprehensive cutting force. Different approaches for the determination of the cutting forces exist in the literature, such as analytical, mechanistic, and numerical [4, 5]. The analysis of cutting force in milling operation can be dated back to Martellotti [6]. Sabberwal et al. [7] correlated the local normal cutting force to the width of the chip by a set of cutting force coefficients. Tlusty and Macneil [8] presented analytical expressions for cutting forces in end-milling operations in which the tangential component of the cutting force was considered to be proportional to the cutting load and the radial force was empirically related to the tangential force. Kline et al. [9] proposed a mechanistic cutting force model by considering the helix face of the cutter as an aggregation of small discrete disks along the axis. Bao and Tansel [10] introduced an analytical cutting force model for micro-milling operations based on the model for conventional milling [8]. Vogler et al [11, 12] have developed a cutting force model for micro-milling that included both the minimum chip-thickness and the microstructure effects. Zaman [13] developed a three-dimensional analytical cutting model for micro-end-milling operation, which determines the theoretical chip area at any specific angular position of the tool cutting edge by considering the geometry of the path of the cutting edge and relates this with tangential cutting force. Lee [14] developed a mechanistic cutting force modeling in micro-end-milling with cutting-condition-independent cutting force coefficients. Lai [15] presented an analytical micro scale milling force model based on the FE simulations using the cutting principles and the slip-line theory. Malekian [16] investigated a mechanistic modeling of micro-milling forces, with consideration of the effects of ploughing, elastic recovery, run-out, and dynamics.

It should be noted that in spite of the extensive research efforts, it is still difficult to model machining, especially micromachining, due to the fact that there are too many variables that need to be taken into account [5]. Mechanistic model is effective in predicting the cutting forces in micro-milling provided that the cutting force coefficients are accurately identified from experiments. However, it is both costly and time-consuming to conduct the cutting experiments. For new combinations of tools and materials without testing data, the cutting forces cannot be predicted using this approach. Theoretically, the cutting forces can be obtained directly from FE simulation. Nevertheless, FEM requires a considerable amount of computational power to produce accurate results. If the analysis using FEM is to consider 3D, special care is needed for simulating a micro-milling process. The degree of complexity and the computational power required are increased, which adds considerably to computational time [5], and thus makes FEM not a practical approach for industrial users.

This paper presents the development of a cutting force model for micro end milling process using a hybrid approach to enable reliable and physically sound prediction of cutting forces in micro-milling without the burden of heavy computational power or experimental work. The proposed cutting force model for micro-end-milling is developed based on a mechanistic cutting force model presented in [17] which was originally for conventional milling processes. In order to further expand the mechanistic cutting force model into micro-milling operation, the effects of the tool cutting edge radius and the minimum uncut chip thickness have to be taken into account. An FEA model is employed to predict the cutting forces in orthogonal micro-cutting by considering the edge radius effect. Based on the FEA simulation results, the cutting force coefficients can be identified. The micro-milling forces are then predicted using the cutting conditions such as the uncut chip thickness and velocity varies. Experimental verification will also be presented.

2. Model development

2.1 General frame of the force model

A schematic diagram of a micro-end-milling cutter is shown in Fig.1. To simplify the model development, the micro-end-milling cutter is divided into a finite number of disk elements with equal axial length *dz* along with the axial axis *Z* of the cutter. The cutting force contributed by a cutting edge segment of the *i*th flute at the *k*th axial disk element at an arbitrary angular position of $\theta(j)$ can be described by the tangential (dF_t), radial (dF_r) and axial (dF_a) cutting force components. Assuming that the cutting force components dF_t, dF_r and dF_a are the sum of a term proportional to the area of cut through a cutting force coefficient K_{tc}, and a term proportional to the width of cut *dz* through the edge coefficient K_{te}, the following equations exist:

$$
\begin{aligned}
dF_t(i,j,k) &= [K_{tc}h(\theta) + K_{te}]dz \\
dF_r(i,j,k) &= [K_{rc}h(\theta) + K_{re}]dz \\
dF_a(i,j,k) &= [K_{ac}h(\theta) + K_{ae}]dz
\end{aligned}
\tag{1}
$$

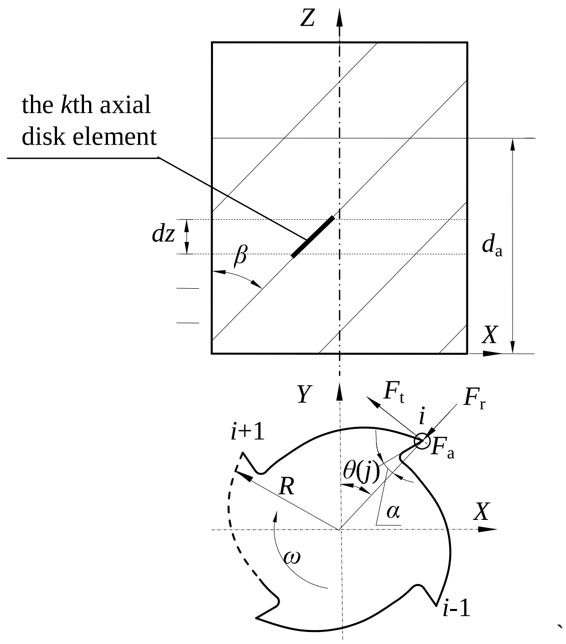

Fig.1 Schematic of micro-end-milling geometry and coordinate

Due to the existence of a helix angle β on the cutter flutes, at a certain instant in time, the cutting action of a flute segment can be regarded as an oblique cutting operation. Based on a mechanistic force model [17], the tangential, radial and axial cutting force coefficients, K_{tc} , K_{rc} , and K_{ac} respectively, which account for shear and friction forces in chip formation, are expressed as

$$K_{tc} = \frac{\tau_s}{sin\emptyset_n} \frac{\cos(\beta_n - \alpha_n) + tan^2\eta sin\beta_n}{\sqrt{\cos^2(\emptyset_n + \beta_n - \alpha_n) + tan^2\eta sin^2\beta_n}}$$

$$K_{rc} = \frac{\tau_s}{sin\emptyset_n cosi} \frac{sin(\beta_n - \alpha_n)}{\sqrt{cos^2(\emptyset_n + \beta_n - \alpha_n) + tan^2\eta sin^2\beta_n}}$$

$$K_{ac} = \frac{\tau_s}{sin\emptyset_n} \frac{\cos(\beta_n - \alpha_n)tan\eta - tan\eta sin\beta_n}{\sqrt{\cos^2(\emptyset_n + \beta_n - \alpha_n) + tan^2\eta sin^2\beta_n}} \quad (2)$$

Where τ_s is the shearing stress, ϕ_n and β_n is the normal shear angle and friction angle respectively, α_n is the normal rake angle, and η is the chip flow angle which is equal to the oblique angle. Traditionally the cutting force coefficients are obtained by evaluating shear angle, friction angle, and shear yield stress from orthogonal cutting tests. Conducting the cutting tests is both costly and time-consuming. For new combinations of tools and materials without testing data in the orthogonal cutting database, the cutting forces cannot be predicted using this model.

To overcome the problems, a hybrid approach is developed in this research. Finite element analysis (FEA) is employed for the determination of the shear stress, shear angle, and friction angle, and then to identify the coefficients K_{tc} , K_{rc} , and K_{ac} based on the work material properties, tool geometry, and the cutting conditions. A series of orthogonal micro-cutting under different cutting conditions are simulated using FEA. The coefficients K_{te} , K_{re} and K_{ae} , which are accounting for the rubbing and ploughing effects at the cutting edge, are calculated by the intercept force components per unit width of force – cut thickness function at zero cut thickness [18].

For micro-milling operation, the tangential, radial and axial forces obtained from Eq.1 can be transformed into the milling coordinates in X, Y, and Z directions, and be expressed as

$$dF_x(i,j,k) = -dF_t cos\theta - dF_r sin\theta$$
$$dF_y(i,j,k) = dF_t sin\theta - dF_r cos\theta$$
$$dF_z(i,j,k) = dF_a \quad (3)$$

The contributions of all cutting edges at the jth angular position are summed up to give the total force components acting on the cutter at any cutter rotation angle θ.

$$F(j) = \sum_k \sum_i F(i,j,k) \quad (4)$$

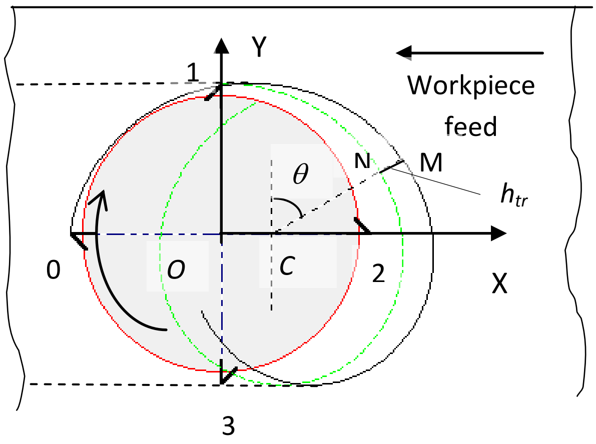

Fig. 2 Uncut chip thickness determination

The cutting force is significantly influenced by the uncut chip thickness. In order to calculate the cutting force in micro-end-milling, the uncut chip thickness has to be accurately computed. In micro-milling with a large ratio of feed per tooth to tool radius, the actual uncut chip thickness is different from that of conventional milling. Li et al. [19] shown that based on the true tooth paths, at a moment during the tool-workpiece engagement in milling, the uncut chip thickness for a cutter tooth engaged in cutting can be determined through finding the intersection point of the path curve left by the preceding tooth and the line passing through the current tooth tip as well as the cutter axis by solving the derived transcendental equation using a numerical method, as in Fig. 2. By using Taylor's series to approximate the involved infinitesimal value in the transcendental equation, an explicit expression for practical determination of the undeformed chip thickness with higher accuracy compared with the traditional model can be determined [19] as

$$h_{tr} = R\left(1-\left(1-\frac{2f_t\sin\phi_i}{r+\frac{N_t f_t}{2\pi}\cos\phi_i}-\frac{f_t^2\cos 2\phi_i}{\left(r+\frac{N_t f_t}{2\pi}\cos\phi_i\right)^2}+\frac{f_t^3\sin\phi_i\cos^2\phi_i}{\left(r+\frac{N_t f_t}{2\pi}\cos\phi_i\right)^3}\right)^{\frac{1}{2}}\right) \qquad (5)$$

Where f_t is the feed per tooth per revolution, N_t is number of teeth, $\phi_j=\theta+j\Delta+\theta_0$ is the instantaneous position angle of the tooth tip analyzed and is measured in *rad* clockwise with reference to the positive *Y*-axis, where θ is the angle of cutter rotation, θ_0 is the initial position angle of this tooth point at the initial time instant $t=0$, and $\Delta = 2\pi/N_t$ is the phase angle between two adjacent teeth.

To take into account the effect of cutter runout, suppose that the cutter has a nominal radius of *r*, the runout of its *i*-th tooth is e_{ri}, then the actual radius of a tooth can be regarded as $r_i' = r + e_{ri}$. It can be shown [20] that the true value of the instantaneous undeformed chip thickness h_{tr} can be determined by

$$\begin{aligned} h_{tr} &= |MN| = |MC| - |NC| \\ &= (r + e_{ri}) - \sqrt{(x_N - x_C)^2 + (y_N - y_C)^2} \end{aligned} \tag{6}$$

Numerical methods have to be used to solve it which has been introduced in [20].

<u>2.2 Size effect in Micro-milling</u>

The most significant characteristics of the micro-cutting operation are the size effect and the minimum uncut chip thickness. It has been found [2] that chip formation does not occur when the uncut chip thickness is less than a minimum chip thickness. In such a case, the effective rake angle that affects the machining process is more negative than the normal rake angle [12]. Fang [21] has introduced the average value of the effective rake angle for understanding the cutting phenomena in micro-cutting. Lee [22] has defined the rake surface by the partial effective rake angle.

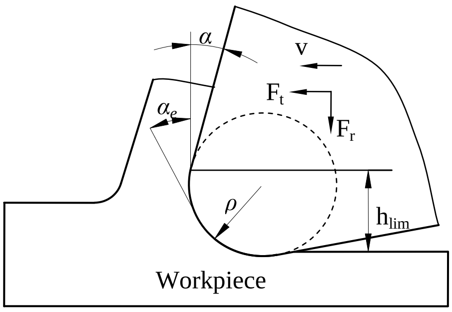

Fig. 3 Edge radius size effect, Equivalent rake angle and rake angle

In order to develop a micro-end-cutting force model, an effective rake angle that will be used to determine the normal and frictional cutting force components is essential. This is shown in Fig. 3. When the uncut chip thickness is less than the height of the tangent point between the rake angle and the arc of the tool edge radius, chip sliding occurs on the nominal rake angle; the partial effective rake angle at a particular point can be formulated as

$$\alpha_e = \begin{cases} -\frac{\pi}{2} + \text{acos}\left(1 - \frac{h}{\rho}\right) & \text{when} \quad h \leq h_{lim} \\ \alpha & \text{when} \quad h > h_{lim} \end{cases} \tag{7}$$

Where h is the uncut chip thickness, ρ is the cutting edge radius, α is the nominal rake angle, and $h_{lim} = \rho(1 + sin\alpha)$ is a limit value of the uncut chip thickness. As an example, the partial effective rake angles of a micro-end-mill with nominal rake angle 6° and edge radius 2μm, respectively, versus different uncut chip thickness, are shown in Fig. 4

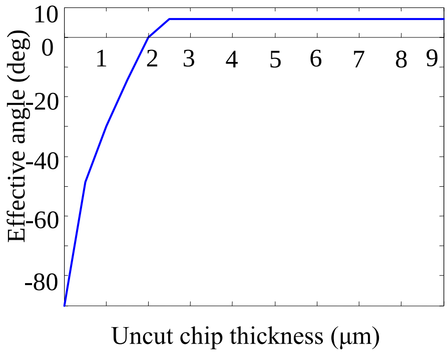

Fig. 4 Effective rake angle with respect to uncut chip thickness

3 Determination of cutting force coefficients

In this study, the cutting forces coefficients are determined based on FE modeling of orthogonal micro-cutting process under different cutting condition. The FE model of orthogonal micro-cutting is developed using the software *Deform3D*. The resultant cutting force coefficients are expressed as nonlinear functions of cutting speed and uncut chip thickness.

3.1 FE model development

A thermo-mechanically coupled FE model of micro-cutting operations is developed by using commercial FE software (Deform). As shown in Fig.3, the tool moves into the workpiece with velocity *v* and the uncut chip thickness *h*. Due to the small size of the tool, the edge shape of the tool has to be taken into consideration. The tool is modeled as a purely rigid body and only heat transfer analysis is taken into consideration for it. The workpiece is modeled as a rectangular block and meshed with four-node thermally coupled tetrahedron element. The nodes of the bottom surface of workpiece are fixed in the cutting and tangential directions. The nodes of the left surface of the worpiece are fixed in the cutting directions. Room temperature (20°C) is applied to both the tool and the workpiece as an initial temperature condition. Arbitrary Lagrangian Eulerian (ALE) adaptive meshing is applied in the FE model to avoid the excessive distortion of the elements. Since remeshing technique is used, there is no need to define the material separation criterion, and excessive distortions of the elements around the tool edge are avoided. Coulomb friction law is used in the current study where a friction coefficient of 0.6 is applied between the workpiece and the tool represented [23].

3.2 Material model

Johnson-Cook constitutive material model [24] is used to represent the elastic-plastic behavior of the workpiece material. The flow stress is dependent on the strain, strain rate, and temperature with the relationship

$$\sigma = (A + B\varepsilon^n)(1 + C\ln\frac{\dot{\varepsilon}}{\dot{\varepsilon}_0})(1 - (\frac{T - T_{room}}{T_m - T_{room}})^m) \quad (8)$$

In this paper, medium-carbon steels are used as the work material. The parameters of the Johnson–Cook constitutive equation for a typical medium-carbon steel, AISI 1045, are given in Table 1. Some mechanical and physical properties of the material are summarized in Table 2.

Table.1 Johnson-cook Parameters of AISI 1045

A(Mpa)	B(Mpa)	n	C	m
553	600	0.234	0.0134	1.0

Table.2 Physical properties of AISI 1045

Elastic Modulus (GPa)	190-210
Poisson's Ratio	0.27-0.30
Density (×1000 kg/m^3)	7.7-8.03
Specific heat capacity(J/Kg. K)	486
Conductivity (W/m^2.K)	50.9

3.3 Prediction of cutting force with the FE model

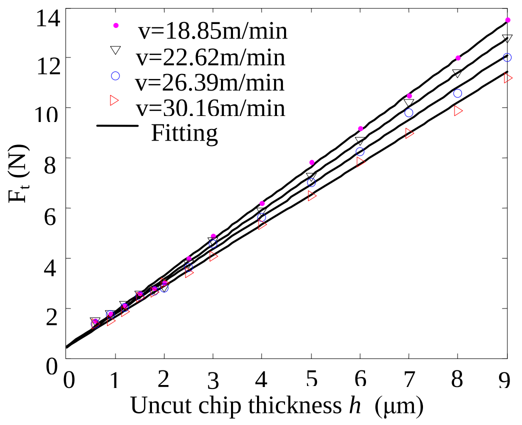

Fig.5 Simulated cutting force in the cutting direction in orthogonal micro-cutting of AISI 1045 steel

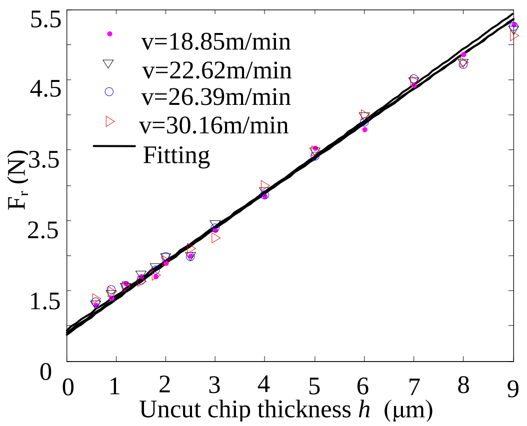

Fig.6 Simulated cutting force in the feed direction in orthogonal micro-cutting of AISI 1045 steel

Cutting forces in orthogonal micro-cutting of AISI 1045 steel are simulated using the FE model. The tool edge radius is defined as 2μm. The nominal tool rake angle is α=10°. Four different cutting speeds are used, including 18.85, 22.62, 26.39, and 30.16 m/min. A series of uncut chip thickness from 0.5 μm to 9 μm are employed in the simulation. The simulated cutting forces in the cutting and feed directions, F_t and F_r, are shown in Figs. 5 and 6 respectively. It can be observed that both F_t and F_r increase along with an increased uncut chip thickness, but the increment rate for F_t is much higher than that for F_r. While a higher cutting speed resulted in a lower F_t, the influence on F_r is very limited. When the uncut chip thickness is small, the workpiece is suppressed downwards by the tool edge which shows a negative effective rake angle between the tool and the workpiece, thus the ploughing force is dominant for very low feed rates. The edge forces are obtained as the intercept at zero uncut chip thickness of the force components from the same orthogonal cutting test.

3.4 Cutting force coefficients

The cutting force coefficients in Eq. 1 will be determined from simulated cutting forces in orthogonal micro cutting using the FE model. With cutting forces (F_t, F_r) obtained, the friction angle and the chip thickness ratio can be derived. The approach to determine the cutting force coefficients is similar to the method for determining the coefficients from experimental cutting tests as introduced in [17]. The edge coefficients are determined from the intercepts of the measured force - uncut chip thickness functions at zero cut thickness from the same orthogonal cutting FE simulation result. The cutting force coefficients are calculated from Eq. (2), and modeled as nonlinear functions of uncut chip thickness and velocity as follows, *t* , *r, a*, represent the directions of tangential, radial, axial respectively:

$$K_{tc} = P_t h^{Qt} + G_t h^{Dt} v^{Et}$$
$$K_{rc} = P_r h^{Qr} + G_r h^{Dr} v^{Er}$$
$$K_{ac} = P_a h^{Qr} + G_a h^{Da} v^{Ea} \quad (9)$$

The parameters of cutting force coefficients in Eq. 9 can be determined from curve-fitting results. The identified parameters are listed in Table.3. As an example, the calculated cutting force coefficients and the fitted curves when the cutting velocity is 30.16 m/min are shown in Fig.7. The relatively large cutting force coefficients for small uncut chip thickness are believed to be caused by the cutting edge effect with significant ploughing.

The minimum chip thickness can be estimated from Fig.7 where the slope of cutting forces coefficient changes more rapidly [14]. In this case, the minimum chip thickness was estimated as about 0.5μm. In order to find out the relationship between the minimum chip thickness and the tool edge radius, chip formation of micro-cutting was also simulated through the FEM, as shown in Fig. 8. It can be observed that when the ratio of the uncut chip thickness to edge radius is 0.2, there is no chip formed, and only material compression and accumulation exist. Chip forms when the ratio is 0.3 or above. From these results, the minimum chip thickness is proposed to be 0.25 times of tool edge radius, which is in fact 0.5μm in this case.

Table.3 Estimated parameters for the cutting coefficients

Index i	*t*	*r*	*a*
P_i	2079.6	966.9	0.4380
Q_i	-0.0976	0	1.3807
G_i	0.01167	1.6867	53.97
D_i	-1.3618	-0.925	-0.711
E_i	0.139	0.330	-0.182

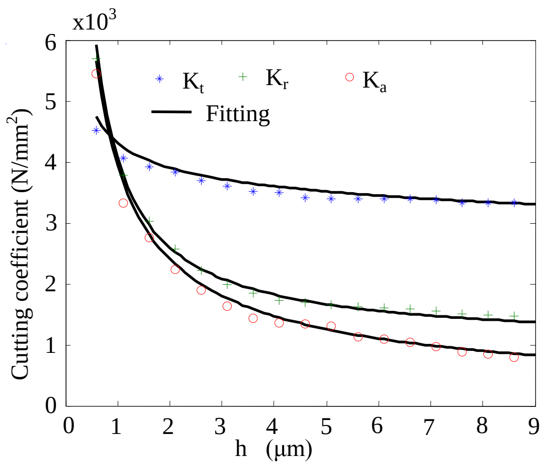

Fig.7 Determined cutting force coefficients with respect to the uncut chip thickness

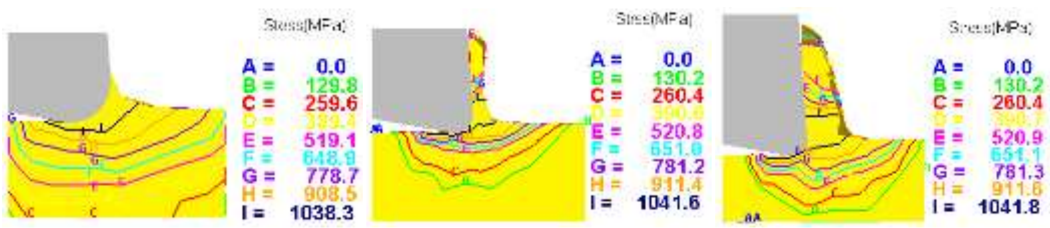

(a) h=0.2ρ (0.6μm) (b) h =0.3ρ (0.9μm) (c) h=ρ (2μm)

Fig. 8 FEM simulation of the chip formation process in orthogonal micro cutting

4. Experimental verification

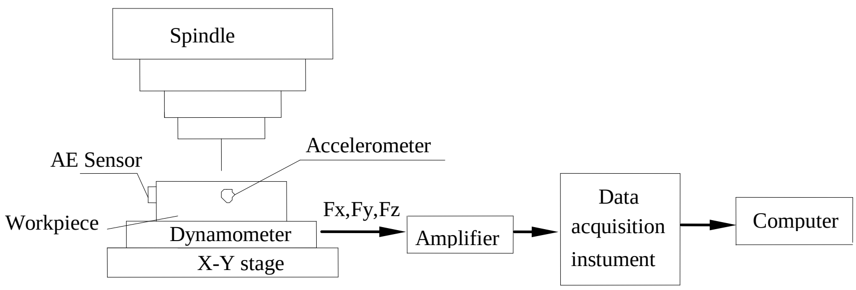

Fig.9 Experimental setup

Fig.10 Microscopic picture of WC micro-mill cutting tool

A Deckel Maho high-speed machining centre with computer numerical control (CNC) was utilized to perform the micro-end milling experiments. The experimental setup is shown in

Fig.9. A medium-carbon steel workpiece was used for the cutting tests. The micro-cutters in this experiment were uncoated tungsten carbide (WC) flat micro-end-mills of 600μm diameter with two flutes. The helix and rake angles were approximately 30° and 10°, respectively. The microscopic picture of the cutter is shown in Fig.10. The measured cutter edge radius of the tool was approximately 3μm. Slot milling was conducted under a constant axial depth of cut of 50 μm. Spindle speeds of 10000rpm, 14000rpm, and 16000rpm were used, which corresponded to cutting speeds of 18.85 m/min, 26.39 m/min, and 30.16 m/min respectively. Feed per tooth values included 0.5, 5, and 7 μm. The cutting forces were measured using a Kistler type 9256C2 dynamometer. The charge signals generated from the force sensor were fed into the kistler 5070 charge amplifier and were converted into voltage signal. A low-pass filter was employed to remove the high-frequency noises in the recorded force signals.

Comparisons of the predicted and measured cutting forces corresponding to five different cutting conditions are illustrated in Figs. 11-15. The prediction of cutting forces was carried out by using the developed cutting force model in this study. It is shown that both the simulation and measured forces have similar variation pattern and closely matched amplitude levels. There are two peaks during one cutter revolution which is caused by the cutting engagement of the two flutes. However, the two peaks are not identical, which is believed to be caused by the cutter run-out and also the cutting process dynamics. In Fig.11 where a low feedrate of 0.5μm/tooth was used, there appears to be only one force peak within one cutter revolution. It can be attributed to a fact that one cutter flute with smaller radius didn't engage in cutting due to the cutter runout and too small feed per tooth. The predicted and the measured forces show the same trends and the peak magnitudes, when cutting speed is lower (see Figs. 11-13). This can be explained that the cutting speed has a noticeable influence on the cutting force with the same feed per tooth; the increase in the cutting speed can lead to an increase in effect of the run out. The cutting forces in X-direction with the proposed models agree well with the experimental results. The discrepancy at the cutting forces in Y-direction is observed between the proposed model and the experiment. This is due to the underestimation of the tangential force from the FE model. It can be seen that the cutter runout and tool-workpiece vibration have a significant effect on the cutting forces, especially at lower feed rates. When the feed per tooth is smaller than the run-out, there is only one cutting edge engaged in the machining operation within one cutter revolution. The effect of cutter runout and vibration should be accounted in future modelling work.

5. Conclusions

A hybrid approach for modeling the cutting force in micro-milling has been presented. The model takes into account the tool geometry, cutting edge radius, work material properties, and cutting parameters such as feed rate, depth of cut and cutting speed. In order to account for the effect of the tool edge radius, an effective rake angle is employed for the determination of the cutting force. By using the proposed approach, the cutting force coefficients are calculated from the FE models and simulations in a more generic way. An FE model of orthogonal cutting has been developed based on the material constitutive model for the determination of the cutting force coefficients. A series of FEA are performed at different cutting conditions. Based on the simulation results, the cutting force coefficients are identified as nonlinear function of uncut chip thickness and cutting parameters. Then the cutting force coefficients are integrated into a mechanistic cutting force model, which can predict cutting forces under different cutting conditions within a very short computational time. The predicted forces using the proposed model have been verified with experimentally measured results at different feed per tooth and cutting speed. The predicted and the measured forces show similar variation pattern and closely matched amplitude levels.

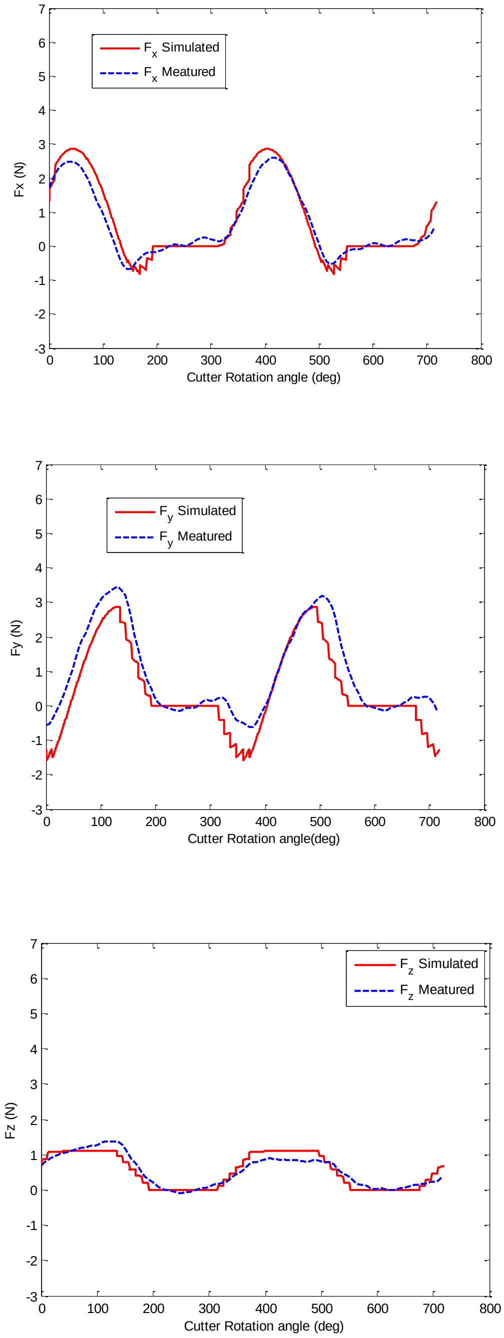

Fig. 11 Comparison of experimental and predicted cutting forces (10000rpm, 0.5μm/tooth)

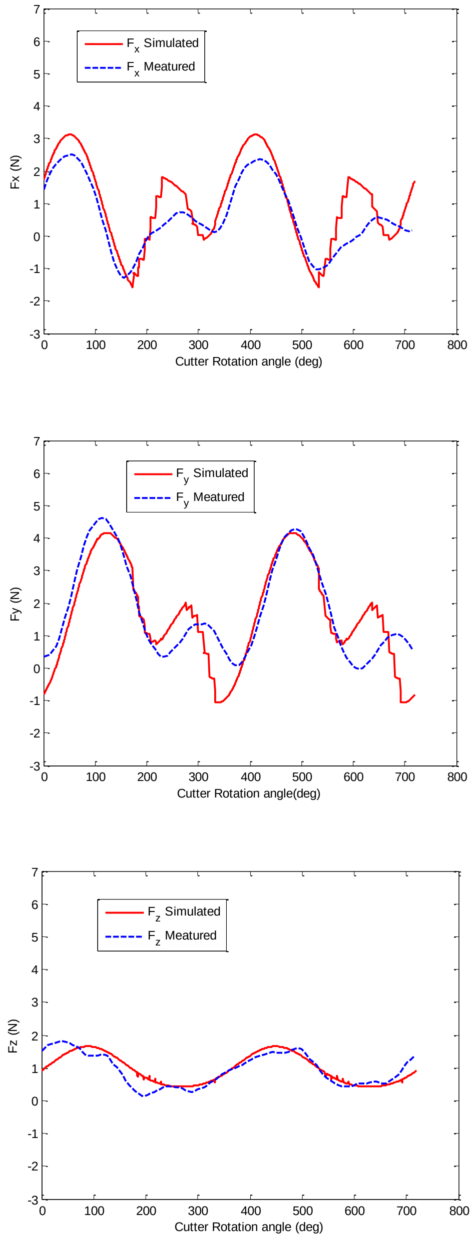

Fig. 12 Comparison of experimental and predicted cutting forces (10000rpm, 5μm/tooth)

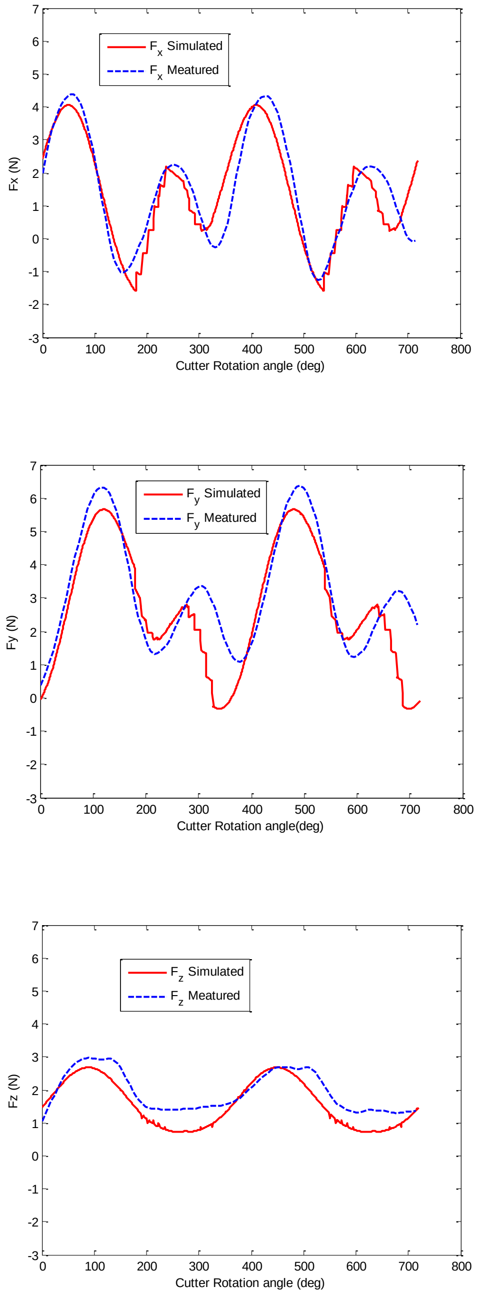

Fig. 13 Comparison of experimental and predicted cutting forces (10000rpm, 7μm/tooth)

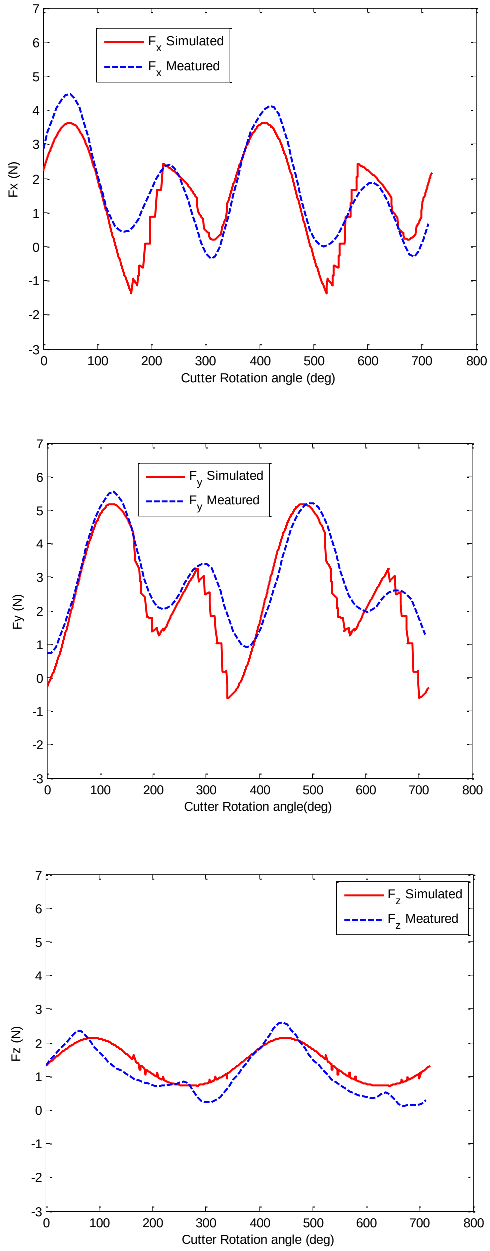

Fig. 14 Comparison of experimental and predicted cutting forces (14000rpm, 5μm/tooth)

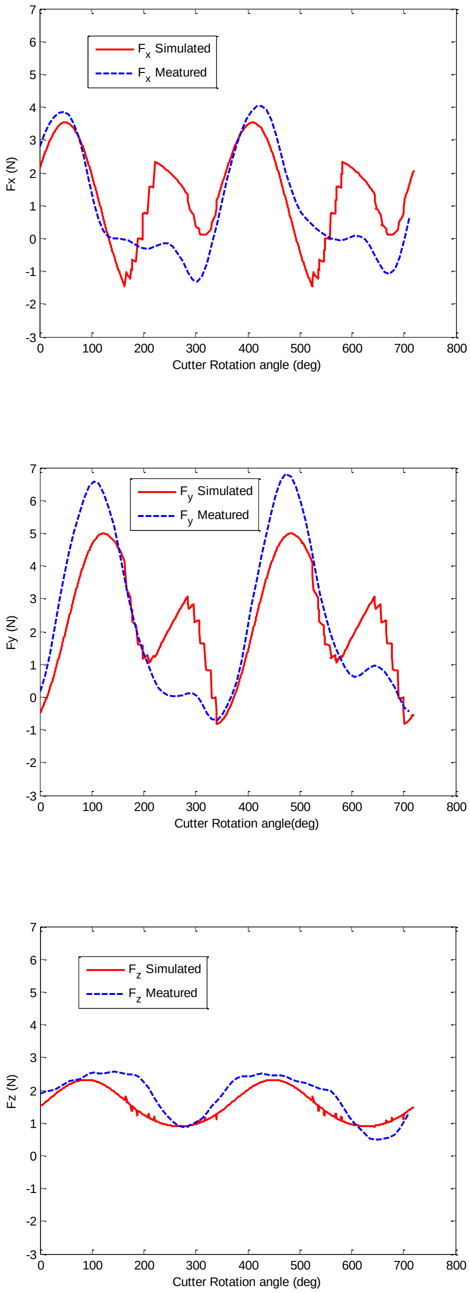

Fig. 15 Comparison of experimental and predicted cutting forces (16000rpm, 5μm/tooth)

Acknowledgments

The first author would like to thank the support to this work by the National Youth Foundation of China (Grant No. 51105270). The work was primarily undertaken at UNSW Australia.

References

[1]. M.J. Vasile, C.R. Friedrich, B. Kikkeri, R.McElhannon, Micrometer-scale machining: tool fabrication and initial results, Precision Engineering, 19, 1999, 180-186.

[2]. H. Weule, V. Huntrup, H. Tritschle, Micro-cutting of steel to meet new requirements in miniaturization, Annals of the CIRP, 50/1, 2001, 61-64.

[3]. J. H. Ko, D. W. Cho, Feed rate scheduling model considering transverse rupture strength of a tool for 3D ball-end milling, International Journal Machine Tools and Manufacture, 44/10, 2004, 1047-1059.

[4]. K. Van Luttervelt, T. H. C. Childs, I. S. Jawahir, F. Klocke, P. K. Venuvinod, Present situation and future trends in modelling of machining operations.CIRP Annals-Manufacturing Technology, 47/2.1998, 587–626.

[5]. A. P. Markopoulos, *Finite Element Method in Machining Processes*, SpringerBriefs in Manufacturing and Surface Engineering, DOI: 10.1007/978-1-4471-4330-7, Springer London Heidelberg New York Dordrecht. 2013

[6]. M.E. Martellotti, An analysis of the milling process, Transaction of ASME 63,1941, 677–700.

[7]. A.J.P. Sabberwal, Chip Section and cutting force during the milling operation, CIRP Annals, 10/3,1961, 62.

[8]. J. Tlusty, P. Macneil, Dynamics of cutting forces in end milling, Annals of CIRP, 24/1, 1975, 21–25.

[9]. W.A. Kline, R.E. DeVor, J.R. Lindberg, The prediction of cutting forces in end milling with application to concerning cuts, IJMTDR 22/1, 1982, 7–22.

[10]. S.M. Afazov, S.M. Ratchev, J. Segal, Modelling and simulation of micro-milling cutting forces, Journal of Materials Processing Technology, 210/15, 2010, 2154–2162.

[11]. M. P. Vogler, R. E. DeVor, and S. G. Kapoor, Microstructure-Level Force Prediction Model for Micro-Milling of Multi-Phase Materials, Journal Manufacturing and Science Engineering, 125/2, 2003, 202–209.

[12]. M. P. Vogler, R. E. DeVor, and S. G. Kapoor, On the Modelling and Analysis of Machining Performance in Micro-Endmilling, Part II: Cutting Force Prediction, Journal Manufacturing and Science Engineering, 126/4, 2004, 695–705.

[13]. M.T. Zaman, A. Senthil Kumar, M. Rahman, S. Sreeram, A three-dimensional analytical cutting force model for micro end milling operation, Journal Machining Tools & Manufacture, 46/3-4,2006,353-366.
[14]. H.U. Lee, D.W. Cho, K.F. Ehmann, A Mechanistic Model of Cutting Forces in Micro-End-Milling With Cutting-Condition-Independent Cutting Force Coefficients, Journal Manufacturing Science and Engineerin,130/3,2008,031102.
[15]. X.M. Lai, H.T. Li, C.F. Li, Z.Q. Lin, J. Ni, Modelling and analysis of micro scale milling considering size effect, micro cutter edge radius and minimum chip thickness. Journal of Machine Tools and Manufacture 48/1: (2008), 1-14.
[16]. Mohammad Malekian, SimonS. Park , MartinB.G. Jun, Modeling of dynamic micro-milling cutting forces, Journal of Machine Tools & Manufacture, 49/7-8, 2009, 586–598.
[17]. Y. Altintas, Manufacturing Automation, Cambridge University Press, 2000
[18]. E. Budak, Y. Altintas, E.J.A. Armarego, Prediction of Milling Force Coefficient From Orthogonal Cutting Data Journal of Manufacturing Science and Engineering, 118/2, 1996, 216 -224.
[19]. H.Z. Li, K. Liu, X.P. Li, A new method for determining the undeformed chip thickness in milling, Journal of Materials Processing Technology, Volume 113, Issues 1–3, 15 June 2001, Pages 378-384.
[20]. H.Z. Li, X.P. Li, A Numerical Study of the Effects of Cutter Runout on Milling Process Geometry Based on True Tooth Trajectory, the International Journal of Advanced Manufacturing Technology. 25: 435-443. (2005)
[21]. F. Z. Fang, Y. C. Liu, On Minimum Exit-Burr in Micro Cutting, Journal Micromechanical and Microengineering, 14/7, 2004, 984–988.
[22]. H.U. Lee, D.W. Cho, K.F. Ehmann, A Mechanistic Model of Cutting Forces in Micro-End-Milling With Cutting-Condition-Independent Cutting Force Coefficients, Journal of Manufacturing Science and Engineering, 130/3,2008,031102.
[23]. P. Sartkulvanich, T. Atlan, Effects of flow stress and friction models in finite element simulation of orthogonal cutting—a sensitivity analysis, Machining Science and Technology, 9/1, 2005, 1–26
[24]. G.R. Johnson, W.H. Cook, A constitutive model and data for metals subjected to large strains, high strain rates and high temperatures. 7th International Symposium on Ballistics, Hague, Netherlands, 1983. 541-547.